Heterogeneous Catalysis

International Edition: DOI: 10.1002/anie.201915526
German Edition: DOI: 10.1002/ange.201915526

Selective Acceptorless Dehydrogenation of Primary Amines to Imines by Core–Shell Cobalt Nanoparticles

Xinjiang Cui[+], Wu Li[+], Kathrin Junge, Zhaofu Fei, Matthias Beller, and Paul J. Dyson**

Abstract: *Core–shell nanocatalysts are attractive due to their versatility and stability. Here, we describe cobalt nanoparticles encapsulated within graphitic shells prepared via the pyrolysis of a cationic poly-ionic liquid (PIL) with a cobalt(II) chloride anion. The resulting material has a core–shell structure that displays excellent activity and selectivity in the self-dehydrogenation and hetero-dehydrogenation of primary amines to their corresponding imines. Furthermore, the catalyst exhibits excellent activity in the synthesis of secondary imines from substrates with various reducible functional groups (C=C, C≡C and C≡N) and amino acid derivatives.*

Introduction

Imines are key intermediates in the synthesis of fine chemicals, pharmaceuticals and natural products.[1–4] Generally, their synthesis involves the direct condensation of an amine and a carbonyl compound.[5,6] Although imines can also be obtained by oxidative dehydrogenation (OD) of primary amines,[7–12] undesired aldehydes and nitriles are also formed as side-products, leading to low selectivities (Scheme 1).[10,13] Consequently, it would be advantageous to eliminate the use of oxidants for this process. Recently, the acceptorless dehydrogenation (AD) of primary amines to imines was shown to be an attractive method for their preparation as fewer side-products are obtained under more inert conditions (with the release of H_2).[14,15] As this reaction is more thermodynamically challenging, the acceptorless dehydrogenation of primary amines has received less attention compared to that of N-heterocycles, with the later reaction having been widely explored for hydrogen storage applications.[16–18]

OD: Oxidant dependent, low selectiviy and limited scope.
AD: High selectivity, but only several homogeneous Ru and heterogeneous Pd catalysts available.

This work:
- ✓ Non-noble cobalt metal used, oxidant and base free;
- ✓ Core-shell structure favoring high selectivy;
- ✓ High yields for homo- and hetero-coupling of primary amines;
- ✓ Good tolerance to reducible groups;
- ✓ Broad substrate scope (31 examples).

Scheme 1. Previous and current work on the dehydrogenation of primary amines to imines.

Acceptorless dehydrogenation of primary amines is usually achieved with molecular catalysts mainly based on Ru.[14,15] However, the aldimine intermediate may undergo a second dehydrogenation to afford a nitrile, which competes with imine formation via a transamination step, resulting in low selectivity of the desired imines. For example, a Ru complex with a P, N-ligand catalyzes the dehydrogenation of benzylamine to imines in only 54% yield because of the formation of the nitrile product.[14]

The acceptorless dehydrogenation of primary amines by heterogeneous catalysts is becoming increasingly attractive because these catalysts tend to be more stable, are easily recycled and are amenable to scale-up for industrial applications. A few heterogeneous systems based on noble metals have been developed for this process. For example, Pd nanoparticles supported on basic hydrotalcites allow the selective synthesis of secondary imines via acceptorless dehydrogenation.[19] In addition, a non-noble metal iron-based catalyst was used to prepare several primary amines via acceptorless dehydrogenation, which is active only in the presence of a strong base (*t*-BuOK).[20] Despite these improvements, the efficient synthesis of imines by acceptorless dehydrogenation of primary amines, especially for hetero-couplings and couplings in the presence of additional reducible groups, remains problematic. Thus, heterogeneous catalysts based on a non-noble metal that efficiently catalyze the oxidant-free and base-free dehydrogenation of primary amines to secondary imines would fulfil an unmet need in organic synthesis.

The unique nature of core–shell nano-structures often leads to improved physical and chemical properties compared to other nanocatalysts, leading to new applications.[21–25] N-doping strategies represent an effective method for the

[*] Dr. X. Cui,[+] Dr. Z. Fei, Prof. P. J. Dyson
Institute of Chemical Sciences and Engineering, École Polytechnique Fédérale de Lausanne (EPFL)
1015 Lausanne (Switzerland)
E-mail: paul.dyson@epfl.ch
Dr. W. Li,[+] Dr. K. Junge, Prof. M. Beller
Leibniz-Institute for Catalysis
Albert Einstein Str. 29a, 18059 Rostock (Germany)
E-mail: matthias.beller@catalysis.de
[+] These authors contributed equally to this work.
Supporting information and the ORCID identification number(s) for the author(s) of this article can be found under https://doi.org/10.1002/anie.201915526.

preparation of selective and active catalysts with numerous advantages demonstrated in photo-, electro- and redox-catalysis.[13,26–31] Here, we describe the preparation, characterization and catalytic evaluation of cobalt-based nanoparticles immobilized within a *N*-doped carbon support. The optimal non-noble metal heterogeneous system catalyzes the acceptorless dehydrogenation of primary amines to secondary imines with unprecedented activities and selectivities (Scheme 1). To the best of our knowledge, non-noble metal-based heterogeneous catalysts have not been reported for the oxidant-free and base-free dehydrogenation of primary amines to imines.

Results and Discussion

The route used to prepare the Co-N/C catalyst is illustrated in Scheme 2, and commences with the synthesis of an imidazolium-based poly-ionic liquid (PIL) with a cobalt-(II) chloride counter anion, followed by its immobilization

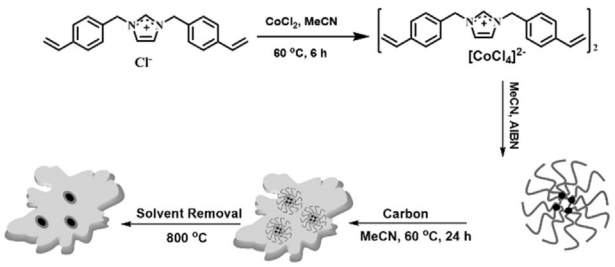

Scheme 2. Preparation of the core–shell cobalt catalyst.

and pyrolysis. In the first step, 1,3-bis(4-vinylbenzyl)imidazolium chloride is obtained according to literature method.[32] The 1,3-bis(4-vinylbenzyl)imidazolium chloride monomer is then reacted with cobalt(II) chloride to afford the monomer containing the $CoCl_4^{2-}$ anion, which is then polymerized in the presence of 2,2′-azobis(2-methylpropionitrile) (AIBN, an initiator). With the addition of carbon support, the resulting slurry was stirred, then dried and pyrolyzed under an argon atmosphere. The most active catalyst, termed Co-N/C-800 was obtained following pyrolysis at 800 °C for 2 h. Other catalysts obtained at different pyrolysis temperatures, that is, 600, 700 and 900 °C were also evaluated. Although this method was expected to promote the formation of a *N*-doped shell during pyrolysis, to the best of our knowledge, *N*-graphene shells have not previously been obtained from PIL templates.

The Co-N/C catalysts were initially characterized by transmission electron microscopy (TEM). As shown in Figures S1–S3, the size of the cobalt nanoparticles increases slightly as the pyrolysis temperature is raised. Following pyrolysis at 800 °C for 2 h, cobalt nanoparticles ranging from 20–50 nm are observed on the surface of the carbon support (Figure S1). The high-resolution TEM (HR-TEM) image shows that the nanoparticles are protected by graphene-like shells (Figures 1 a–c), comprising typically 3–12 layers with a thickness of 1.2–3.0 nm. Presumably, carbonization of the

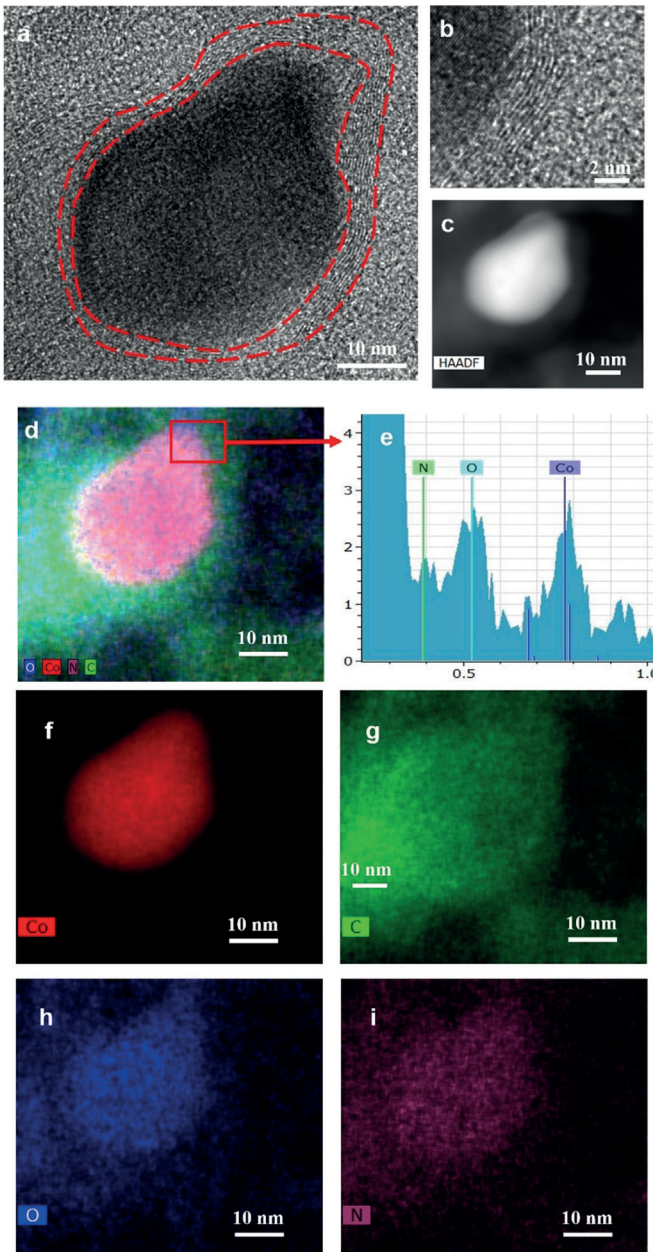

Figure 1. Characterization of the Co-N/C-800 catalyst: (a) Bright field TEM image; (b) HR-TEM image; (c) HAADF-STEM image; TEM-EDS mapping images: (d) overlap; (e) EDX spectrum; (f) Co; (g) C; (h) O; (i) N.

nitrogen-containing PIL leads to the formation of nitrogen-doped graphene-like shells. Nanoscale element mapping (Figures 1 d,f–i) reveals that the cobalt is concentrated in the core region, whereas C, N and O are distributed throughout the entire particle, confirming the core–shell structure. The composition of the nanostructures were further investigated by energy-dispersive X-ray (EDX) spectroscopy, with N, O and Co detected (see Figure 1 e). In contrast, a Co/C-800 catalyst prepared in the absence of the PIL was aggregated with nanoparticles > 200 nm (Figure. S5) that do not possess a core–shell, indicating that the formation of the core–shell structure inhibits nanoparticle aggregation.

ICP-OES (inductively coupled plasma–optical emission spectrometry) and XPS (X-ray photoelectron spectroscopy) analysis show that the carbon content increases with the pyrolysis temperature, whereas the content of N and Co decreases (Tables S1 and S2). The content of the Co drops from 2.7 to 1.8% as the pyrolysis temperature increases from 600 to 800°C and the N decreases from 4.10 to 2.43%. However, upon increasing the temperature to 900°C, the content of Co and N decrease sharply to 0.35 and 0.81%, respectively. The peaks in the N 1s spectrum at 398.6, 400.5 and 401.6 eV may be tentatively assigned to pyridinic, pyrrolic and graphitic N on the basis of their respective binding energies (Figure 2b).[33,34] The percentage of pyridine-type nitrogen decreases as the pyrolysis temperature increases whereas the pyrrolic and graphitic N-species increase with the pyrolysis temperature (Table S3). In addition, Co^0, Co–O and Co–N species are present, evidenced by the binding energies at 779.1, 780.4, and 783.1 eV after pyrolysis at 800°C (Figure 2a and Table S4). The presence of Co–O bonds might be due to the retention of oxygen in the carbon support or the surface Co atoms being partially oxidized when the catalysts are exposed to air after pyrolysis. Upon increasing the pyrolysis temperature from 600 to 800°C, the content of Co–O bonds decreases from 72 to 48% whereas the Co–N bonds increase from 19 to 31% (Table S4). In addition, the percentage of Co^0 increases from 9 to 22% as the pyrolysis temperature is increased from 600 to 800°C (Table S4). At 900°C the contents of Co^0 and Co–N species decreases to 9 and 15%, respectively. Taken together, in the Co-N/C-800 catalyst the main active sites are likely to be based on CoNx units.

XRD analysis was used to probe the structure of the catalysts (see Figure 2c), with diffraction peaks observed at 36.7 and 44.1° in all the catalysts, which are close to the (101) and (111) planes of CoOx and CoNx units, respectively.[33] Stronger and sharper diffraction peaks are observed in the Co-N/C-800 catalyst, implying higher ordering and crystallinity in this material. In the Co-N/C-900 catalyst, the peak corresponding to the Co–O component is of higher intensity than in the other samples, whereas the peak corresponding to the Co–N species is very low, consistent with the XPS data. As shown in Figure 2d, the diffraction peak at 44.5° could be due to the (111) plane of Co^0 in the Co/C-800 catalyst, close in value to the Co–N peak. Notably, the pyrolysis temperature and the PIL exert a significant influence on the formation of active sites.[33]

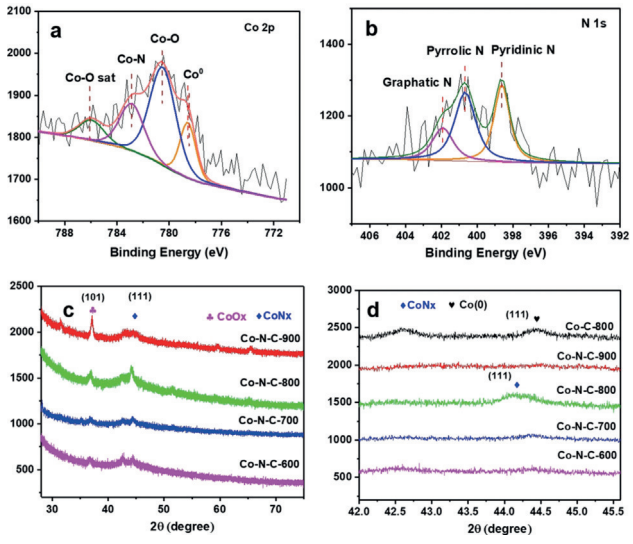

Figure 2. XPS spectra for the (a) Co 2p and (b) N 1s of the Co-N/C-800 catalyst. (c) XRD patterns of the Co-N/C-600, Co-N/C-700, Co-N/C-800 and Co-N/C-900 catalysts. (d) Partial XRD patterns of the Co-N/C-600, Co-N/C-700, Co-N/C-800, Co-N/C-900 and Co/C-800 materials.

The catalytic dehydrogenation of 4-methoxybenzylamine (**1a**) was chosen as benchmark reaction to evaluate and optimize catalytic performance (Table 1). The catalyst prepared at 600°C is the least active of the Co-N/C catalysts affording N-(4-methoxybenzylidene)-4-methoxybenzylamine (**2a**) in 71% yield (Table 1, entry 1). The activity of the Co-N/C-700 and Co-N/C-800 are considerably higher with almost quantitative yields of corresponding imine obtained in toluene for the latter (Table 1, entries 2–3).

In comparison, the Co/C-800 control catalyst without core–shell structure affords the desired product in only 21% yield (Table 1, entry 4), with the secondary amine obtained in 8% yield, indicating that the core–shell structure in Co-N/C-800 inhibits the over-reduction of C=N bonds leading to high selectivity. Note that the Co-N/C-900 catalyst is less active than the Co-N/C-800 catalyst (Table 1, entry 5), possibly due

Table 1: Optimization of the self-dehydrogenation of 4-methoxybenzylamine.[a]

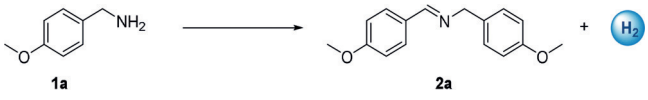

1a **2a**

Entry	Catalyst	Solvent	*t* [h]	Yield [%][b]	Sel. [%]	TON
1	Co-N/C-600	Toluene	12	71	99	118.3
2	Co-N/C-700	Toluene	12	93	99	155.0
3	Co-N/C-800	Toluene	12	99	99	165.0
4	Co/C-800	Toluene	12	21	72	35
5	Co-N/C-900	Toluene	12	85	98	141.7
6	Co-N/C-800	Xylene	12	86	98	143.3
7	Co-N/C-800	Dioxane	12	75	99	125.0
8	Co-N/C-800	Water	12	81	99	135.0
9	Co-N/C-800	Butyldiglycol	12	84	99	140.0
10	Co-N/C-800	Toluene	6	67	99	111.7
11	Co-N/C-800	Toluene	10	84	99	140.0
12	Co-N/C-800	Toluene	16	98	99	163.3
13	Co-N/C-800	Toluene	24	98	99	163.3
14	Co-N/Al_2O_3-800	Toluene	12	81	99	135.0
15	Co-N/SiO_2-800	Toluene	12	67	99	111.7
16	$CoCl_2$	Toluene	12	22	99	36.7
17	$CoCl_2$ + C	Toluene	12	29	99	48.3
18	$CoCl_2$ + N/C	Toluene	12	34	99	56.7
19	Pd/C	Toluene	12	65	67	108.3
20	Pt/C	Toluene	12	52	53	86.7
21	Ru/C	Toluene	12	39	41	65.0
22	Co-N/C-800[c]	Toluene	12	56	99	93.4

[a] Reaction conditions: catalyst (0.6 mol% of Co relative to the substrate), 4-methoxybenzylamine (0.2 mmol), solvent (1 mL), N_2 atmosphere, 120°C. [b] GC yield. TON = mol product mol^{-1} Co. [c] The catalyst was treated under air.

to the presence of fewer Co–N sites. To confirm this hypothesis, the catalyst was further treated at 250 °C for 2 h under air, with the resulting catalyst displaying an even lower yield (Table 1, entry 22). ICP-OES analysis showed the N content decreased sharply (Table S1). These results suggest that the selectivity of the dehydrogenation may be attributed to the core–shell structure, whereas the Co–N units act as the active sites enhancing the reaction rate.

Next, different solvents including xylene, dioxane, water and butyl digol were evaluated in the model reaction at 120 °C, giving yields in the range 75–86 % (Table 1, entries 6–9) with 99 % selectivity, that is, lower than the yield obtained in toluene. As expected, the yield is lower at shorter reaction times (Table 1, entries 10 and 11), whereas the N-alkylated amine is no longer observed following prolonged reaction times (Table 1, entries 12 and 13), showing that hydrogenation of C=N bond cannot take place, which leads to the high selectivity observed. Low catalytic activity was obtained using Co-N/Al_2O_3-800and Co-N/SiO_2-800 as supported catalysts (Table 1, entries 14 and 15). The catalytic activity of $CoCl_2$ in the presence of the carbon and N-doped carbon was also very low (Table 1, entries 16–18). Remarkably, the performance of the Co-N/C-800 catalyst is even superior to that of commercial noble metal catalysts (Pd/C, Pt/C and Ru/C), due to the formation of N-alkylated amine with these catalysts leading to 41–67 % of selectivity (Table 1, entries 19–21).

From the reaction profile as shown in Figure 3, in which nitrile formation is not observed, it would appear that the transamination step is much faster than the second dehydrogenation of the aldimine intermediate, which differs to the reactivity observed for homogeneous catalysts.[35,36] After 12 h, the imine was obtained in 96 % yield. Importantly, there is no evidence for the formation of the N-alkylated secondary amine and tertiary amine, resulting from the further hydrogenation of the imine using the released hydrogen, which are detected in reactions employing other heterogeneous[19] and homogeneous catalysts.[37] The imine is stable beyond 12 h, implying the reverse hydrogenation is not possible.

The reaction was studied in situ by ^{1}H-NMR spectroscopy, and over time the signals corresponding to the 4-methoxybenzylamine -CH_2 group (**a** in Figure 3) decrease and the peaks corresponding to the -CH_2 group (**b** in Figure 3) of the product increase. Moreover, the proton signal at 8.13 ppm corresponding to the HC=N proton (**c** in Figure 3) also increases with time. Note that release of H_2 was detected by gas chromatography (Figure S8). The stability and recyclability of the Co-N/C-800 catalyst were also established. After each reaction, the Co-N/C-800 catalyst was recovered by centrifugation and the product quantified. The catalytic transformation of **1a** to **2a** could be repeated multiple times (Figure 4). High selectivity was retained although the conversion decreased from 99 % to 90 % over six batches. XPS analysis revealed that the amount of Co–N bonds decreased to 26 % after the recycling, leading to the loss of the conversion (Figure S7), further confirming the role of these bonds (see above). However, the core–shell structure remains intact and hence the selectivity of the Co-N/C-800 catalyst remains unchanged (Figure S4).

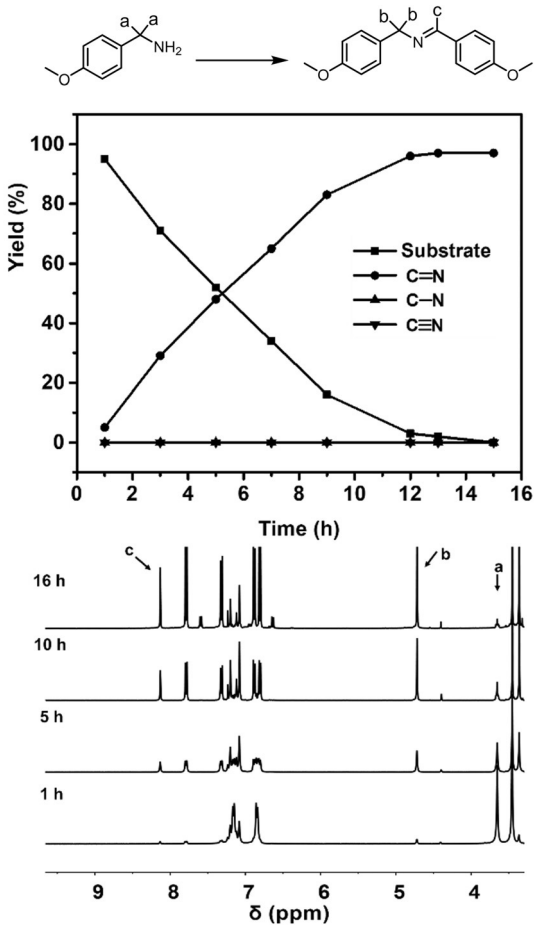

Figure 3. Reaction profile for dehydrogenative coupling of 4-methoxybenzylamine to afford the imine (C=N), secondary amine (C-N) and nitrile (C≡N) using a 0.6 mol % loading of the Co-N/C-800 catalyst (top). In-situ ^{1}H-NMR spectra of the self-dehydrogenation of 4-methoxybenzylamine using a 1.0 mol % loading of the Co-N/C-800 catalyst under the optimized reaction conditions in tolunene-d8 (bottom).

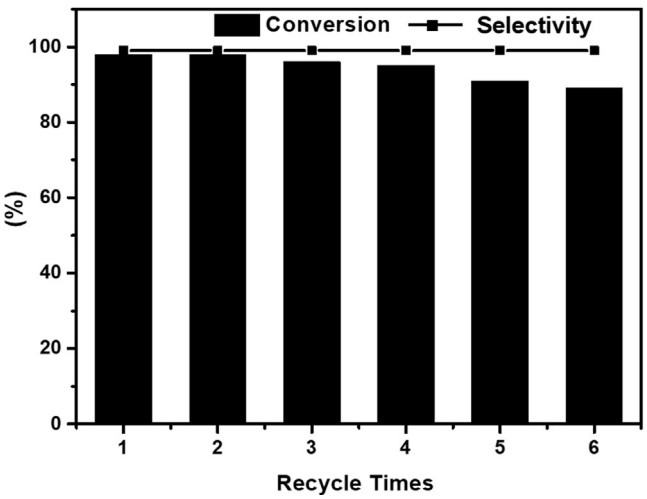

Figure 4. Recycling of Co-N/C-800 catalyst in the dehydrogenation of **1a**. Reaction conditions: **1a** (0.2 mmol), toluene (1 mL), N_2 atmosphere, 120 °C, 16 h.

Since the Co-N/C-800 catalyst displayed the best activity in the acceptorless dehydrogenation of 4-methoxybenzylamine (**1a**) to the corresponding imine (**2a**), the scope of the reaction was studied using this catalyst under the optimized conditions. As shown in Table 2, 3-methoxybenzylamine (**1b**) was converted to the corresponding imine in 93% yield (Table 2, entry 2). However, 2-methoxybenzylamine (**1c**), which has a more sterically hindered functional group, is converted to the corresponding imine in 91% yield with a reaction time to 24 h (Table 2, entry 3). As expected, in the case of 3,4-dimethoxybenzylamine, a high yield was achieved using the Co-N/C-800 catalyst (Table 2, entry 4). Substituted benzylamines with electron-donating ester, methyl or isopropyl groups at the *para*-position, were converted to the corresponding imines in high yields by extending the reaction time (Table 2, entries 5–7). Although benzylamine (**1h**) and substrates (**1i, 1j**) with electron-withdrawing functional groups (F and Cl) are less reactive, high yields can still be achieved by prolonging the reaction time to 48 h without the substrates undergoing dehalogenation (Table 2, entries 8–10). In contrast, 2-thiophenemethylamine (**1k**) was dehydrogenated to the corresponding imine in 95% yield (Table 2, entry 11). However, a yield of only 46% was observed for the dehydrogenation of 2-picolyamine **1l** (Table 2, entry 12). Notably, bio-based primary amines such as furfurylamine (**1m**) and 5-methyl furfurylamine (**1n**) were transformed to the corresponding imines in 88 and 86% yield, respectively (Table 2, entries 13 and 14). Remarkably, **2o** was obtained by the self-dehydrogenation of n-octylamine in 87% yield without the formation of a nitrile or N-alkylated amine (Table 2, entry 15).[10,13] This methodology offers a straightforward approach to aromatic and aliphatic imines under the oxidant- and base-free conditions.

Table 2: Co-N/C-800 catalyzed self-dehydrogenation of primary amines.[a]

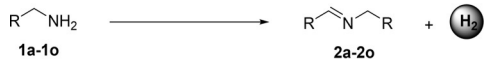

Entry	Substrate		Product		*t* [h]	Yield [%][b]
1	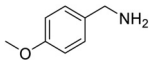	**1a**	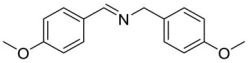	**2a**	12	99(91)
2	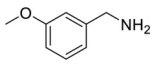	**1b**	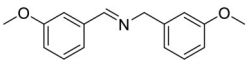	**2b**	15	93(85)
3	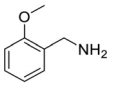	**1c**	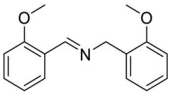	**2c**	24	91
4	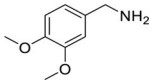	**1d**	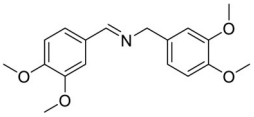	**2d**	12	97
5	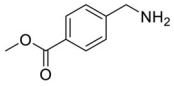	**1e**	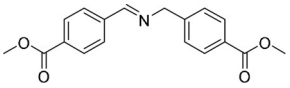	**2e**	16	94
6	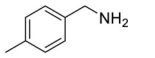	**1f**	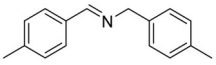	**2f**	28	91(83)
7	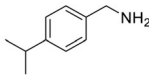	**1g**	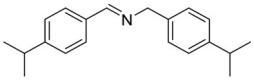	**2g**	24	97
8	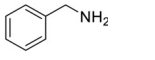	**1h**	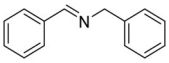	**2h**	48	89
9	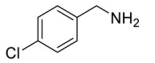	**1i**	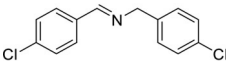	**2i**	48	96
10	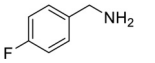	**1j**	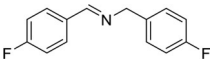	**2j**	48	97(90)
11	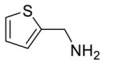	**1k**	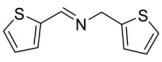	**2k**	30	95
12	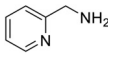	**1l**	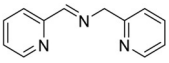	**2l**	30	46[c]
13	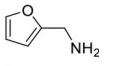	**1m**	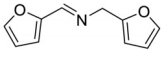	**2m**	24	88
14	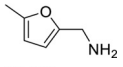	**1n**	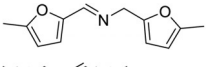	**2n**	24	86
15	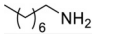	**1o**	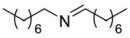	**2o**	48	87(78)

[a] Reaction conditions: catalyst (0.6 mol% of Co to substrate), amine (0.2 mmol), toluene (1 mL), N_2 atmosphere, 120°C, H_2 yield in parentheses. [b] Isolated yields. [c] ^{1}H-NMR spectroscopic yield.

After demonstrating the activity of the catalyst towards a broad range of primary amines, the catalyst was used to explore the catalytic acceptorless hetero-coupling of different amines (Table 3). The catalytic dehydrogenation of 4-methoxybenzylamine (**1a**) with other amines was initially explored. Using 1-phenylethylamine (**3a**) and 2-phenylethylamine (**3b**), the reaction proceeds with complete consumption of 4-methoxybenzylamine, affording the hetero-coupled products in 74 and 84% yield, respectively (Table 3, entries 1–2). Note that excess amines are needed to afford the desired products in high yield. Moreover, after hetero-dehydrogenation, **4c** and **4d** were successfully prepared in 84% and 97% yields, respectively, from the corresponding aliphatic amines (Table 3, entries 3–4). High yields were also achieved using cyclohexanamine (**3e**) and cyclopentanamine (**3f**) in the presence of the Co-N/C-800 catalyst (Table 3, entries 5–6). N-arylimines were obtained in high yield when using anilines as reactants, irrespective of whether they have electron-withdrawing (F or I) or electron-donating (methyl) substituents, illustrating the utility of anilines in the hetero-dehydrogenation reaction (Table 3, entries 7–10). Note that the **1a** can be fully converted in all cases in the presence of Co-N/C-800, however the self-dehydrogenation of **1a** was not avoided leading to the lower yields of the desired hetero-dehydrogenated imines.

As molecular hydrogen is released during the reaction, we decided to investigate whether other reducible functional groups would be compatible with the catalyst. As shown in Figure S9, self-dehydrogenation of 4-methoxyl benzylamine was achieved in high yield in the presence of compounds with reducible groups, demonstrating the tolerance to reducible functional groups. Conse-

Table 3: Hetero-dehydrogenation of primary amines using the Co-N/C-800 catalyst.[a]

Entry	Substrate		Product		*t* [h]	Yield [%][b]
1	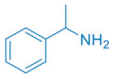	**3a**	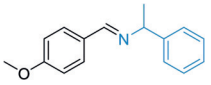	**4a**	24	74
2	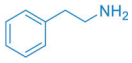	**3b**	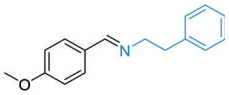	**4b**	24	84
3		**3c**	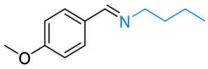	**4c**	24	97
4	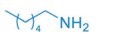	**3d**	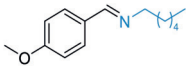	**4d**	24	84
5	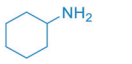	**3e**	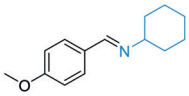	**4e**	18	94
6	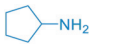	**3f**	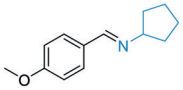	**4f**	18	95
7	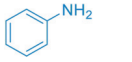	**3g**	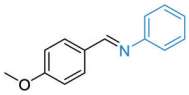	**4g**	20	67
8	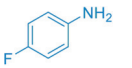	**3h**	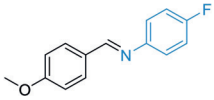	**4h**	20	78
9	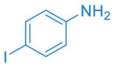	**3i**	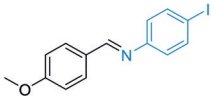	**4i**	20	75
10	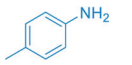	**3j**	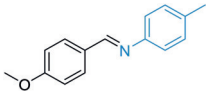	**4j**	20	79

[a] Reaction conditions: catalyst (0.6 mol% of Co to substrate), 4-methoxybenzylamine (0.2 mmol), **3a**–**3j** (0.3 mmol), toluene (1 mL), N_2 atmosphere, 120°C. [b] ^{1}H-NMR spectroscopic yields based on **1a**.

quently, we explored the application of the Co-N/C-800 catalyst in the synthesis of several imines bearing reducible groups (Scheme 3). Notably, imines containing C=C bonds can be obtained selectively by the self-dehydrogenation of amines. Imines bearing C≡C and C≡N groups (**5b** and **5c**) can also be prepared via self-coupling without the reduction of these groups. Using 4-nitroaniline, hetero-coupling of the desired product imine (**5d**) with n-octylamine can be achieved. To the best of our knowledge, such dehydrogenations have not been described previously and, therefore, this method is powerful for the further functionalization of substituted imines.

Applications of amino acids derivatives that can be derived from biomass α-hydroxyl acids are particularly attractive.[38–41] Consequently, we investigated the hetero-dehydrogenation of primary amines with amino acids derivatives. As shown in Scheme 4, in the presence of 1.5 equivalents of hexylamine or octylamine, methyl 2-amino-2-

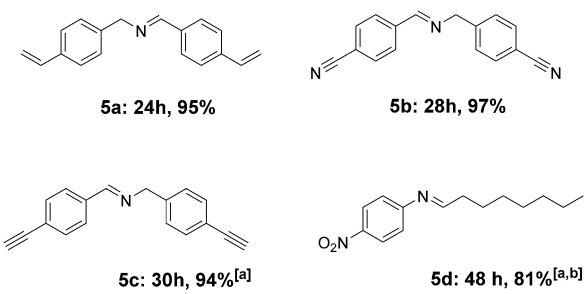

Scheme 3. Dehydrogenation of primary amines with reducible groups using the Co-N/C-800 catalyst. Reaction conditions: catalyst (0.6 mol% of Co to substrate), primary amine (0.2 mmol), toluene (1 mL), N_2 atmosphere, 120°C. [a] ^{1}H-NMR spectroscopic yield, [b] n-octylamine (0.3 mmol).

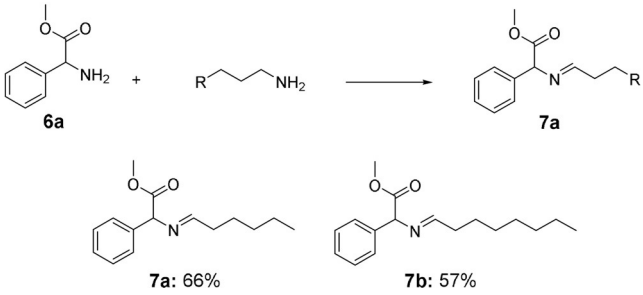

Scheme 4. Dehydrogenation of primary amines with amino-acid derivatives. Reaction conditions: catalyst (1.0 mol% of Co to substrate), phenylglycine methyl ether (0.2 mmol), amine (0.3 mmol), toluene (1 mL), N_2 atmosphere, 120°C, 18 h, ^{1}H-NMR spectroscopic yield.

phenylacetate was converted to the corresponding products (**7a/b**) in 66% and 57% yield, respectively.

The synthetic utility of secondary imines was also probed under practical conditions. As shown in Scheme 5, N-benzylideneaniline was successfully transformed into the corresponding product (**8a**) in 65% yield following reaction with allyltrimethylsilane. Cross-coupling of N-benzylidenebenzylamine and 1-pentyne was also achieved in 70% yield to afford **8b**.

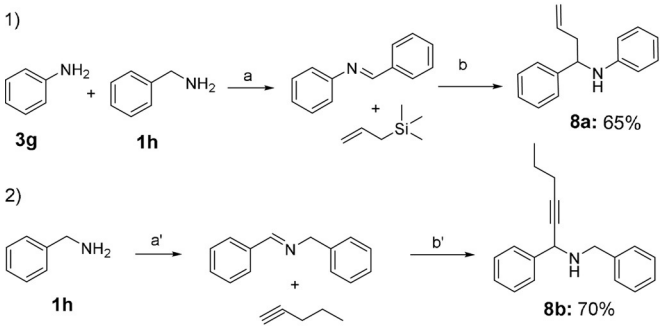

Scheme 5. Further reactions of imines. Reaction conditions: a) catalyst (0.6 mol% of Co to substrate, toluene, 48 h. b) Allyltrimethylsilane (0.6 mmol), imine (0.5 mmol), 4 Å molecular sieves (150 mg), TBAF (5 mol%) and THF (2 mL), 70°C, 18 h, yield based on **3g**. a') As shown in Table 2. b') Imine (0.5 mmol), alkyne (0.75 mmol), $Cu(OTf)_2$ (1 mol%), Na_2SO_4, toluene (2 mL), 100°C, 24 h. yield based on **1h**.

Conclusion

Herein we described a new method for the synthesis of nanostructured nitrogen-doped graphene-layer coated cobalt nanoparticle catalysts immobilized on a carbon support. The resulting core–shell catalysts are easily obtained in a simple and scalable way via pyrolysis of a PIL with an appropriate metal halide anion, in this case $CoCl_4^{2-}$. The optimized catalyst was used in the selective self-dehydrogenation of primary amines to secondary imines, in the hetero-coupling of different amines to the corresponding imines. The utility of the catalyst is highlighted by the synthesis of imines with reducible groups and amino acids derivatives.

Acknowledgements

We thank the EPFL, Swiss National Science Foundation and the Swiss Competence Center for Energy Research (SCCER) for Heat and Electricity Storage for financial support. We also thank Pierre Mettraux and Lagrange Thomas for analytical support.

Conflict of interest

The authors declare no conflict of interest.

Keywords: amines · cobalt · dehydrogenation · heterogeneous catalysis · imines

How to cite: *Angew. Chem. Int. Ed.* **2020**, *59*, 7501 – 7507
Angew. Chem. **2020**, *132*, 7571 – 7577

[1] K. Weissermel, H.-J. Arpel, *Industrial Organic Chemistry*, Wiley-VCH, Weinheim, **2003**, pp. 59 – 89.
[2] P. F. Ji, K. Manna, Z. Lin, X. Y. Feng, A. Urban, Y. Song, W. B. Lin, *J. Am. Chem. Soc.* **2017**, *139*, 7004 – 7011.
[3] P. F. Ji, K. Manna, Z. K. Lin, A. Urban, F. X. Greene, G. X. Lan, W. B. Lin, *J. Am. Chem. Soc.* **2016**, *138*, 12234 – 12242.
[4] B. S. Takale, X. J. Feng, Y. Lu, M. Bao, T. A. Jin, T. Minato, Y. Yamamoto, *J. Am. Chem. Soc.* **2016**, *138*, 10356 – 10364.
[5] S. Kobayashi, Y. Mori, J. S. Fossey, M. M. Salter, *Chem. Rev.* **2011**, *111*, 2626 – 2704.
[6] S. Kobayashi, H. Ishitani, *Chem. Rev.* **1999**, *99*, 1069 – 1094.
[7] B. Chen, L. Y. Wang, W. Dai, S. S. Shang, Y. Lv, S. Gao, *ACS Catal.* **2015**, *5*, 2788 – 2794.
[8] J. L. Long, K. Shen, Y. W. Li, *ACS Catal.* **2017**, *7*, 275 – 284.
[9] K. Z. Wang, P. B. Jiang, M. Yang, P. Ma, J. H. Qin, X. K. Huang, L. Ma, R. Li, *Green Chem.* **2019**, *21*, 2448 – 2461.
[10] X. J. Lang, H. W. Ji, C. C. Chen, W. H. Ma, J. C. Zhao, *Angew. Chem. Int. Ed.* **2011**, *50*, 3934 – 3937; *Angew. Chem.* **2011**, *123*, 4020 – 4023.
[11] Z. Y. Zhai, X. N. Guo, G. Q. Jin, X. Y. Guo, *Catal. Sci. Technol.* **2015**, *5*, 4202 – 4207.
[12] X. J. Lang, W. H. Ma, Y. B. Zhao, C. C. Chen, H. W. Ji, J. C. Zhao, *Chem. Eur. J.* **2012**, *18*, 2624 – 2631.
[13] R. V. Jagadeesh, H. Junge, M. Beller, *Nat. Commun.* **2014**, *5*, 4123 – 4131.
[14] J. M. Stubbs, R. J. Hazlehurst, P. D. Boyle, J. M. Blacquiere, *Organometallics* **2017**, *36*, 1692 – 1698.
[15] L. P. He, T. Chen, D. R. Gong, Z. P. Lai, K. W. Huang, *Organometallics* **2012**, *31*, 5208 – 5211.
[16] S. Chakraborty, W. W. Brennessel, W. D. Jones, *J. Am. Chem. Soc.* **2014**, *136*, 8564 – 8567.
[17] D. Talwar, A. Gonzalez-de-Castro, H. Y. Li, J. L. Xiao, *Angew. Chem. Int. Ed.* **2015**, *54*, 5223 – 5227; *Angew. Chem.* **2015**, *127*, 5312 – 5316.
[18] W. B. Yao, Y. X. Zhang, X. Q. Jia, Z. Huang, *Angew. Chem. Int. Ed.* **2014**, *53*, 1390 – 1394; *Angew. Chem.* **2014**, *126*, 1414 – 1418.
[19] D. Ainembabazi, N. An, J. C. Manayil, K. Wilson, A. F. Lee, A. M. Voutchkova-Kostal, *ACS Catal.* **2019**, *9*, 1055 – 1065.
[20] G. Jaiswal, V. G. Landge, D. Jagadeesan, E. Balaraman, *Nat. Commun.* **2017**, *8*, 2147 – 2159.
[21] L. Z. Bu, N. Zhang, S. J. Guo, X. Zhang, J. Li, J. L. Yao, T. Wu, G. Lu, J. Y. Ma, D. Su, X. Q. Huang, *Science* **2016**, *354*, 1410 – 1414.
[22] T. Mitsudome, M. Yamamoto, Z. Maeno, T. Mizugaki, K. Jitsukawa, K. Kaneda, *J. Am. Chem. Soc.* **2015**, *137*, 13452 – 13455.
[23] Q. Li, J. J. Fu, W. L. Zhu, Z. Z. Chen, B. Shen, L. H. Wu, Z. Xi, T. Y. Wang, G. Lu, J. J. Zhu, S. H. Sun, *J. Am. Chem. Soc.* **2017**, *139*, 4290 – 4293.
[24] H. L. Jiang, T. Akita, T. Ishida, M. Haruta, Q. Xu, *J. Am. Chem. Soc.* **2011**, *133*, 1304 – 1306.
[25] S. Alayoglu, B. Eichhorn, *J. Am. Chem. Soc.* **2008**, *130*, 17479 – 17486.
[26] R. W. Mo, D. Rooney, K. N. Sun, H. Y. Yang, *Nat. Commun.* **2017**, *8*, 13949 – 13957.
[27] Y. Pan, K. A. Sun, S. J. Liu, X. Cao, K. L. Wu, W. C. Cheong, Z. Chen, Y. Wang, Y. Li, Y. Q. Liu, D. S. Wang, Q. Peng, C. Chen, Y. D. Li, *J. Am. Chem. Soc.* **2018**, *140*, 2610 – 2618.
[28] Y. Hou, T. Z. Huang, Z. H. Wen, S. Mao, S. M. Cui, J. H. Chen, *Adv. Energy Mater.* **2014**, *4*, 1400337 – 1400344.
[29] K. Shen, L. Chen, J. L. Long, W. Zhong, Y. W. Li, *ACS Catal.* **2015**, *5*, 5264 – 5271.
[30] R. V. Jagadeesh, A. E. Surkus, H. Junge, M. M. Pohl, J. Radnik, J. Rabeah, H. M. Huan, V. Schunemann, A. Bruckner, M. Beller, *Science* **2013**, *342*, 1073 – 1076.
[31] F. A. Westerhaus, R. V. Jagadeesh, G. Wienhofer, M. M. Pohl, J. Radnik, A. E. Surkus, J. Rabeah, K. Junge, H. Junge, M. Nielsen, A. Bruckner, M. Beller, *Nat. Chem.* **2013**, *5*, 537 – 543.
[32] C. Fu, L. Meng, Q. Lu, Z. Fei, P. J. Dyson, *Adv. Funct. Mater.* **2008**, *18*, 857 – 864.
[33] X. H. Liu, L. J. Xu, G. Y. Xu, W. D. Jia, Y. F. Ma, Y. Zhang, *ACS Catal.* **2016**, *6*, 7611 – 7620.
[34] C. H. Tang, A. E. Surkus, F. Chen, M. M. Pohl, G. Agostini, M. Schneider, H. Junge, M. Beller, *Angew. Chem. Int. Ed.* **2017**, *56*, 16616 – 16620; *Angew. Chem.* **2017**, *129*, 16843 – 16847.
[35] I. Dutta, S. Yadav, A. Sarbajna, S. De, M. Holscher, W. Leitner, J. K. Bera, *J. Am. Chem. Soc.* **2018**, *140*, 8662 – 8666.
[36] K. N. T. Tseng, A. M. Rizzi, N. K. Szymczak, *J. Am. Chem. Soc.* **2013**, *135*, 16352 – 16355.
[37] G. E. Dobereiner, R. H. Crabtree, *Chem. Rev.* **2010**, *110*, 681 – 703.
[38] W. P. Deng, Y. Z. Wang, S. Zhang, K. M. Gupta, M. J. Hulsey, H. Asakura, L. M. Liu, Y. Han, E. M. Karp, G. T. Beckham, P. J. Dyson, J. W. Jiang, T. Tanaka, Y. Wang, N. Yan, *Proc. Natl. Acad. Sci. USA* **2018**, *115*, 5093 – 5098.
[39] J. Paradowska, M. Stodulski, J. Mlynarski, *Angew. Chem. Int. Ed.* **2009**, *48*, 4288 – 4297; *Angew. Chem.* **2009**, *121*, 4352 – 4362.
[40] T. Yan, B. L. Feringa, K. Barta, *Sci. Adv.* **2017**, *3*, eaao6494 – eaao6500.
[41] P. Hu, Y. Ben-David, D. Milstein, *J. Am. Chem. Soc.* **2016**, *138*, 6143 – 6146.

Manuscript received: December 5, 2019
Revised manuscript received: January 16, 2020
Accepted manuscript online: February 12, 2020
Version of record online: March 11, 2020

